Modelling and Simulation Reveals Density-Dependent Re-Entry Risk in the Infarcted Ventricles After Stem Cell-Derived Cardiomyocyte Delivery

Leto L Riebel[1], Zhinuo J Wang[1], Hector Martinez-Navarro[1], Cristian Trovato[1], Jacopo Biasetti[2], Rafael Sachetto Oliveira[3], Rodrigo Weber dos Santos[4], Blanca Rodriguez[1]

[1]Department of Computer Science, University of Oxford, Oxford, United Kingdom
[2]AstraZeneca AB R&D, Molndal, Sweden
[3]Universidade Federal de São João del-Rei, São João del-Rei, Brazil
[4]Universidade Federal de Juiz de Fora, Juiz de Fora, Brazil

Abstract

Delivery of human pluripotent stem cell-derived cardiomyocytes (hPSC-CMs) is a potential therapy to improve cardiac function after injury. However, hPSC-CMs express immature electrophysiological and structural properties and may be pro-arrhythmic.

Our goal is to identify key factors determining arrhythmic risk of hPSC-CM therapy in the infarcted human ventricles through modelling and simulation. We model three densities of hPSC-CMs covering 4%, 22%, and 39% of the infarct and border zone and induce re-entry through ectopic stimulation. We furthermore simulate the effect of different therapeutic agents on re-entry susceptibility.

Due to the increased refractory period of the hPSC-CMs, the vulnerable window increases from 20ms in control, to 60ms in the low- and 80ms in the medium- and high-density scenarios. Our results highlight the density-dependent effect of hPSC-CM delivery on arrhythmic risk after myocardial infarction and show the effect of therapeutic strategies on this increased re-entry susceptibility.

1. Introduction

Cardiovascular disease, such as myocardial infarction (MI), is the leading cause of death worldwide. While studies have shown the ability of the human heart to regenerate [1], this happens at a slow rate, insufficient to restore cardiac function after injury. To reverse or at least halt myocardial damage, delivery of hPSC-CMs is investigated as a therapeutic option. Stem cells and stem cell-derived cardiomyocytes have been injected intramyocardially in experimental studies [2] and cultured into tissue patches later transplanted into the human heart clinically and experimentally [3, 4]. While hPSC-CMs show promising capabilities, they exhibit immature structure and function. Properties such as slow upstroke velocity, increased action potential (AP) duration, and reduced conduction velocity might provide a pro-arrhythmic substrate when the cells are introduced into the adult human heart. Non-fatal arrhythmias have indeed been observed experimentally after hPSC-CM delivery [5].

Modelling and simulation can offer unique insights into arrhythmia mechanisms and the safety of different delivery configurations. In this study, we use modelling and simulation to determine the arrhythmic risk of different hPSC-CM delivery densities in the infarcted human ventricles. Additionally, we model the effect of four therapeutic strategies and assess their ability to prevent re-entry in the pro-arrhythmic high-density scenario.

2. Methods

Electrophysiological activity is simulated using a biventricular human-based model building from single cell membrane kinetics to tissue conductivities [6]. Model parameters are altered within the infarct and hPSC-CM region. A left anterior infarct with 75% transmurality and a border zone with a maximum width of 0.5cm is introduced [6]. Healthy conduction velocity is set to 65, 31, and 17cm/s in the longitudinal, transverse, and sheet normal direction, respectively as measured in [7] and reduced in the infarct and border zone by 66%.

Mesh elements are tagged as hPSC-CMs by sampling from a normal distribution taking the infarct centre on the endocardium as the mean, a standard deviation of 1cm, and a cut-off radius of 2.5cm. Low, medium, and high densities are modelled by varying the sampling size and transmurality and cover 4, 22 and 39% of the infarct and border zone (see Figure 1). Isotropic conduction velocity of 10cm/s is set for the hPSC-CMs, in line with experimentally recorded ranges [8]. Simulations are run using a monodomain model discretised with the finite volume method [9] and linear hexahedral elements with an edge length of 0.5mm.

The ToR-ORd [10] and Paci2020 [11] models are used to simulate the adult human ventricular, and ventricular-like hPSC-CM AP, respectively. Electrophysiological remodelling at acute stage post-MI in the infarct and border zone is modelled by scaling time constants and conductances of the fast sodium current (I_{NaF}), transient outward potassium current (I_{to}), inward rectifier potassium current (I_{K1}), rapid and slow delayed outward rectifier potassium currents (I_{Kr}, I_{Ks}), L-type calcium current (I_{CaL}) and background calcium current (I_{Cab}), as established in [6] and summarised in Table 1.

Scaling factors	IZ	BZ
G_{NaF}	0.40	0.38
G_{to}	0.00	
P_{Ca}	0.64	0.31
P_{Cab}	1.33	
G_{Kr}	0.70	0.30
G_{K1}	0.60	
G_{Ks}		0.20
aCaMK	1.50	
tau_{relp}	6.00	
Conduction Velocity	0.33	0.33

Table 1: Scaling factors for simulating myocardial infarction in the infarct zone (IZ), and border zone (BZ) as in [6].

To reach steady state, three 1Hz beats are simulated and followed by an ectopic stimulus on the healthy endocardial surface proximal to the border zone at 360, 380, 400, 420, 440, 460, and 480ms after the last sinus activation. Re-entry susceptibility is measured as the window during which re-entry is inducible (vulnerable window).

Drug action of cisapride, verapamil, nitrendipine, and lidocaine is modelled as in [12] under 1 x maximal effective free therapeutic concentration ($EFTPC_{max}$) with drug-induced current conductance changes computed using the simple-pore block model [13] (see Table 2).

3. Results

Our results, as summarised in Figure 2, show that the vulnerable window in the infarcted control (with no hPSC-CMs), and low-density scenarios, is 20ms and 60ms long, respectively. The vulnerable window further increases to 80ms in both the medium-, and high-density scenarios. While in the medium-density scenario the vulnerable window ranges from 380 to 460ms after the last sinus beat, it is shifted to 400 to 480ms in the high-density scenario.

The prolonged vulnerable window across the different densities is explained by the source-sink mismatch. The hPSC-CMs present a source with elevated diastolic membrane potential, increased AP duration (APD), and longer refractory period compared to the infarcted adult tissue they replaced (see Figure 3). Repolarisation times in the centre of the hPSC-CM region increase by 50ms in low-density and by 130ms in high-density compared with the infarct zone in the control simulations (360ms). This accounts for a delay in re-excitability and the wider vulnerability window in the high- vs low-density simulations. The repolarisation time in the high-density hPSC-CM scenario is close to the APD at 90% repolarisation of 480ms in the single cell hPSC-CM Paci2020 model.

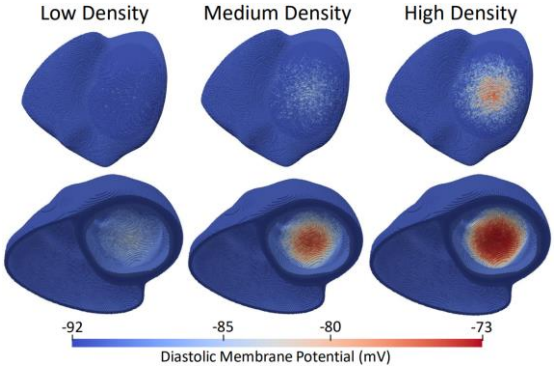

Figure 1: *In-silico* diastolic membrane potential of low (left column), medium (middle column), and high (right column) hPSC-CM densities.

Drug	G_{NaF}	G_{Kr}	G_{CaL}	G_{NaL}	G_{Ks}	G_{K1}
Cisapride		0.858				
Verapamil	0.985	0.932	0.522	0.995	0.998	0.990
Nitrendipine		0.999	0.839			
Lidocaine	0.935	0.991		0.864		

Table 2: Ionic current conductance scaling factors for four drugs under 1 x $EFTPC_{max}$ [12] using a simple-pore block model [13].

	360	380	400	420	440	460	480
Control	--	-	+	-	-	-	-
Low Density	--	+	+	+	-	-	-
Medium Density	--	+	+	+	+	-	-
High Density	--	--	+	+	+	+	-

Figure 2: Vulnerable windows for ectopic beats applied 360 to 480 ms after the last sinus beat for different hPSC-CM densities. A yellow box with a plus sign (+) marks a re-entry, while a blue box with a minus sign (-) means no re-entry is observed. A grey box with a double minus sign (--) indicates that the ectopic stimulus did not propagate.

The increased hPSC-CM repolarisation times cause an increase in local repolarisation dispersion around the injection site, thus elevating re-entry susceptibility. This is illustrated in Figure 4, where the APs proximal to the ectopic stimulus location in the medium- and high-density scenarios are compared. The hPSC-CMs in the high-density scenario exhibit a more depolarised diastolic potential and longer APD under sinus rhythm than in the

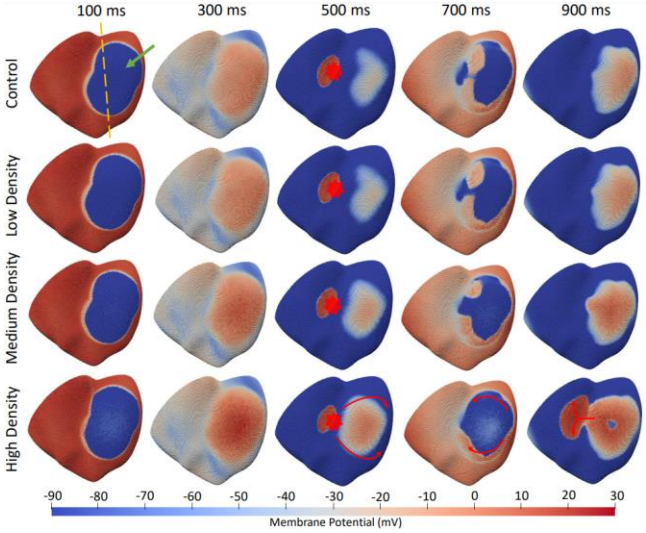

Figure 3: Electrical propagation through the infarcted human-based biventricular model in control and following the introduction of hPSC-CMs at low, medium, and high densities (with 4, 22, and 39% of infarct and border zones replaced, respectively). The green arrow in the top left points at the infarct zone in the left ventricle marking the centre of hPSC-CM delivery. The yellow dotted line represents the axis between the right and left ventricle. Re-entry is established following an ectopic stimulus applied at the endocardium proximal to the border zone at 460ms after the last sinus beat, indicated by the red star. The red arrows highlight the re-entry path.

lower density scenarios, resulting in the ectopic beat to cause a diminished AP at the site of the ectopic stimulus in the high-density scenario. Hence, when the wave propagates around and then through the infarct and hPSC-CM region, the cells can be stimulated again allowing for retrograde propagation, as shown in Figure 3.

Increased hPSC-CM APD and refractory time not only cause a prolongation of the vulnerable window, but also for the ectopic stimulus applied at 380ms after the last sinus beat in the high-density scenario to not propagate at all, as the tissue at the site of the ectopic stimulus is still refractory. Hence, while the length of the vulnerable window is maintained, its onset is delayed compared to the medium-density scenario. In the injection centre of the high-density scenario, the depolarised resting membrane potential of -73mV as represented by the hPSC-CM single cell model is preserved. In the medium- and low-density scenario the diastolic membrane potential decreases to -75 and -84mV, respectively, due to the more negative resting membrane potential of the surrounding adult tissue acting as an electrotonic sink.

Figure 5 shows the effect of four different therapeutic strategies, namely cisapride, lidocaine, nitrendipine, and verapamil, on the re-entry inducibility in the high-density scenario. Application of nitrendipine and lidocaine has little effect on the APD and does not alter the vulnerable window. Cisapride, due to I_{Kr}-block induced APD prolongation, causes a delay of the vulnerable window but does not impact its length. In contrast, application of verapamil shortens the APD due to I_{CaL}-block, which promotes the propagation of the ectopic stimulus through the infarcted tissue at earlier ectopic stimulus times.

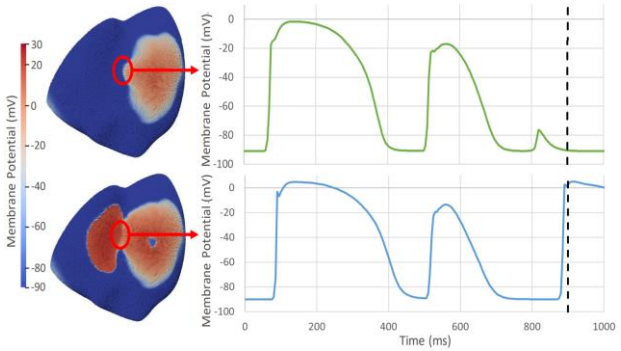

Figure 4: The images on the left show the membrane potential in the medium (top) and high (bottom) hPSC-CM density scenario at 900ms after the last sinus beat. The red circle indicates where an ectopic stimulus is applied on the endocardial surface at 460ms after the last sinus beat. On the right, APs at the ectopic stimulus site for the medium (top row, green) and high (bottom row, blue) density scenarios are shown. The first AP is under sinus rhythm, while the second is initiated through the ectopic stimulus. Only in the high-density scenario a third AP is triggered caused by the ectopic stimulus re-entering through the hPSC-CM area. The black dashed line indicates the time shown in the images on the left.

	360	380	400	420	440	460	480
High Density	--	--	+	+	+	+	-
+ Cisapride	--	--	--	+	+	+	+
+ Lidocaine	--	--	+	+	+	+	-
+ Nitrendipine	--	--	+	+	+	+	-
+ Verapamil	--	+	+	+	+	+	-

Figure 5: Vulnerable windows for an ectopic beat occurring 360, 380, 400, 420, 440, 460, and 480ms after the last sinus beat for different drugs applied to the high-density scenario. A yellow box with a plus sign (+) marks a re-entry, a blue box with a minus sign (-) means no re-entry is observed, and a grey box with a double minus sign (--) indicates that the ectopic stimulus did not propagate.

4. Discussion

Here, using our 3D human-based computational modelling and simulation framework, we have shown a density-dependent arrhythmic risk of hPSC-CM delivery. We show that re-entry risk is higher after hPSC-CM delivery and increases for greater hPSC-CM densities. In our framework, we propose a novel strategy to model the delivery of hPSC-CMs with respect to their density and make use of state-of-the-art single cell models tested thoroughly against experimental data. Due to its multiscale nature, our framework allows for detailed investigation of arrhythmia mechanisms.

Experimental studies show that improvements in left ventricular function in a guinea pig model after cardiac

injury were only achieved for sufficiently high doses [14]. Therefore, while a high dose of hPSC-CMs seems necessary, it may also be arrhythmogenic, as shown in our study. Another *in silico* study examined the effect of density, clustering, and location on hPSC-CM automaticity, concluding that higher cell doses promote ectopic propagation [15]. No spontaneous activity occurs in our biventricular simulations. While a high hPSC-CM density causes a more depolarised resting membrane potential in the hPSC-CM region increasing the spontaneous beating rate to about 0.6Hz, this is suppressed by the 1 Hz sinus beat.

Our results modelling drug effects show that none of the tested drugs reduce the vulnerable window which is most sensitive to I_{Kr} and I_{CaL} block. Length of the vulnerable window is largely maintained although the application of cisapride delays its onset. Verapamil increases the length of the vulnerable window while also bringing forward its onset. Further simulations are needed to explore more drugs and doses. Recently, *in silico* simulations in tissue slabs suggested that addressing the slow upstroke velocity and depolarised diastolic potential in hPSC-CMs may increase therapy efficiency without increasing the arrhythmic risk [16]. Hence, a sodium current agonist could provide a promising solution to increase conduction velocity and, subsequently, minimise the repolarisation gradient and re-entry susceptibility.

5. Conclusion

Our simulations conclude that re-entry susceptibility in our infarcted *in silico* human-based biventricular model depends on the hPSC-CM density and is sensitive to I_{Kr} and I_{CaL} block. We also show that *in silico* simulations can provide a detailed tool to investigate hPSC-CM delivery parameters and contribute to identifying maximal efficacy whilst ensuring minimal arrhythmic risk.

Acknowledgments

This project was funded by a BBSRC PhD scholarship in collaboration with AstraZeneca (BB/V509395/1) to LR. BR holds a Wellcome Trust Senior Research Fellowship in Basic Biomedical Sciences (214290/Z/18/Z) and an NC3Rs Infrastructure for Impact Award (NC/P001076/1). The Paci2020 model was provided by Dr. Michelangelo Paci and the Computational Biophysics and Imaging Group (CBIG) at Tampere University Foundation. We also would like to thank UFJF, UFSJ, CNPq and Fapemig.

References

[1] O. Bergmann et al., “Evidence for cardiomyocyte renewal in humans”, *Science*, vol. 324, no. 5923, pp. 98-102, Apr. 2009.

[2] K.A. Gerbin et al., “Enhanced electrical integration of engineered human myocardium via intramyocardial versus epicardial delivery in infarcted rat hearts”, *PLoS ONE*, 10(7):e0131446, Jul. 2015.

[3] P. Menasché et al., “Transplantation of human embryonic stem cell–derived cardiovascular progenitors for severe ischemic left ventricular dysfunction”, *J. Am. Coll. Cardiol*, vol. 71, no. 4, pp. 429-438, Jan. 2018.

[4] J. Yokoyama et al., “Human induced pluripotent stem cell-derived three-dimensional cardiomyocyte tissues ameliorate the rat ischemic myocardium by remodeling the extracellular matrix and cardiac protein phenotype”, *PLoS ONE*, 16(3):e0245571, Mar. 2021.

[5] J.J.H. Chong et al., “Human embryonic stem-cell-derived cardiomyocytes regenerate non-human primate hearts”, *Nature*, 510:273-277, Apr. 2014.

[6] X. Zhou, Z. J. Wang et al., “Ionic remodelling following myocardial infarction explains phenotypic variability in ECG and arrhythmic substrate but not in ejection fraction”, *bioRxiv*, doi: 10.1101/2022.02.15.480392, 2022.

[7] B. J. Caldwell et al., “Three distinct directions of intramural activation reveal nonuniform side-to-side electrical coupling of ventricular myocytes”, *Circ Arrhythm Electrophysiol.*, 2(4):433-440, Aug. 2009.

[8] J. Hansen et al., “Development of a contractile cardiac fiber from pluripotent stem cell derived cardiomyocytes”, *Front Cardiovasc Med.*, 5:52, Jun. 2018

[9] R. Sachetto Oliveira et al., “Performance evaluation of GPU parallelization, space-time adaptive algorithms, and their combination for simulating cardiac electrophysiology”, *Int J Numer Methods Biomed Engng.*, 34:e2913, Feb. 2018.

[10] J. Tomek et al., “Development, calibration, and validation of a novel human ventricular myocyte model in health, disease, and drug block”, *eLife 2019*, 8:e48890, Dec. 2019.

[11] M. Paci et al., “All-optical electrophysiology refines populations of in silico human iPSC-CMs for drug evaluation”, *Biophys J.*, vol. 118, no. 10, pp. 2596-2611, May 2020.

[12] E. Passini et al., “Human in silico drug trials demonstrate higher accuracy than animal models in predicting clinical pro-arrhythmic cardiotoxicity”, *Front Physiol.*, vol. 8, Sept. 2017.

[13] T. Brennan et al., “Multiscale modelling of drug-induced effects on cardiac electrophysiological activity”, *Pharm Sci.*, vol. 36, no. 1, pp. 62-77, Jan. 2009.

[14] E. Querdel et al., “Human engineered heart tissue patches remuscularize the injured heart in a dose-dependent manner”, *Circulation*, 143(20):1991-2006, Mar. 2021.

[15] J.K. Yu et al., “A comprehensive, multiscale framework for evaluation of arrhythmias arising from cell therapy in the whole post-myocardial infarcted heart”, *Sci Rep 9*, Jun. 2019.

[16] D. Fassina et al., “Modelling the interaction between stem cells derived cardiomyocytes patches and host myocardium to aid non-arrhythmic engineered heart tissue design”, *PLoS Comput. Biol.*, 18(4):e1010030, Apr. 2022.

Address for correspondence:

Leto L Riebel
Department of Computer Science, Wolfson Building, Parks Road, Oxford, OX1 3QD (UK)
leto.riebel@gtc.ox.ac.uk